Analysis and Optimization of Erosive Wear of Al 6113 Age- hardened Alloy: Taguchi and Desirability Function Approach

Pradeep NB[a], Harsha HM[b], Manjunath Patel GC[c*], Ajith BS[d]

[a]Dept. of Mechanical Engineering, JNN College of Engineering, Shivamogga, Affiliated to Visvesvaraya Technological University, Belagavi, India, [b]Dept. of Mechanical Engineering, GM Institute of Technology, Davanagere, Affiliated to Visvesvaraya Technological University, Belagavi, India, [c]Dept. of Mechanical Engineering, PES Institute of Technology and Management, Shivamogga, Affiliated to Visvesvaraya Technological University, Belagavi, India, [d]Department of Mechanical Engineering, Sahyadri College of Engineering and Management, Mangaluru, Affiliated to Visvesvaraya Technological University, Belagavi, India

[*]Corresponding Author Email: manju09mpm05@gmail.com

Abstract: Erosion is a commonly encountered problem in various industrial (such as chemical, cement, thermal power plants, mining and mineral processing) parts, wherein the parts undergo progressive loss of material due to mechanical and chemical interactions among the solid surface and a fluid. Speed, height, and duration are the critical parameters influence the erosive wear (EW). Taguchi L_{27} orthogonal array experiments were conducted to study the parameters that influence on erosive wear of specimen located at three different angles (0^o, 45^o and 90^o). Age-hardened Al 6113 alloy specimen was prepared according to ASTM G67 standard and examined the EW. Experiments are carried out in a rotating slurry (5% HCL+ 20% Al_2O_3 + H_2O) tank with a specimen located at three different angles. Impact speed found to have maximum contribution followed by scissor jack height and time. Note that, scissor jack height and time found to have linear relationship with EW. The EW was expressed as a mathematical function of input variables (impact speed, scissor jack height and time). The EW models developed for all specimens mounted at different angles resulted with better correlation coefficient with a value greater than 0.9. Desirability function approach (DFA) estimated optimal input variables set resulted with a minimum value of erosive wear equal to 0.5258 gm, when the specimen located at an angle 90^0. Furthermore, multi-objective optimization was carried out to estimate the single set of input variables towards minimum EW for all specimens mounted at different angles.

Keywords: Al 6113 age-hardened alloy, Erosive wear, Impact speed, Scissor jack heightand Time.

1.0 Introduction

In today's vast material library, Aluminium (Al) and its alloy still being used in aerospace, defense, marine and automotive appliances [Davis, 1993]. The wide spread of applications are due to the intrinsic properties such as corrosion resistance, lightweight, low density, high strength to weight ratio, toughness, and strength [Dursun & Soutis (2014)]. In general, mechanical parts are subjected to relative motion among the solid surfaces and a contacting substance results in progressive loss of part materials causes wear [Kumar et al. (2011)]. Erosion also results in progressive loss of parent material (i.e. original) occurs because of mechanical interaction among the mating surface and single or multi-elemental fluid or

striking of solid or liquid particles [Prashanth, 2020]. Mechanical/structural parts such as blades (helicopter, impeller), transportation viz. pipes (slurry, oil), hydro turbine (boiler tubes, pump, propellers in an oil and gas industries), earth movers working in mining environments and so on, must possess better erosion resistance to function reliably without catastrophic failure [Prashanth, 2020; Kiragi et al. 2019]. Hence, the study of erosive wear behavior to meet the stringent requirements for specific applications of parts fabricated with alluminium alloy is of paramount importance.

Erosion phenomenon is a complex process influenced by variables such as, erodent particles and its size, impingement angle, material properties (hardness, strength, toughness, and so on), deformation, carrier medium (fluid properties), impact speed or velocity, erodent feed rate, and so on [Kiragi et al. 2019; Prashanth, 2020; Kiragi et al. 2019a]. Desale et al. showed that the size of erodent particles influences both kinetic energy and wear [Desale et al. 2009]. It was observed that smaller size particles possess lower striking efficiency and kinetic energy in comparison with bigger size erodent particles causes less wear. It was also observed that hardness and wear have direct relationship among themselves [Patel et al. 2020; Harsha et al. 2008]. The angular location of cylindrical specimens, particle size and energy in a slurry-pot erosion testing equipment influences the EW [Clark et al. 1995; Elmidany et al. 2020]. Kumar et al. reported that material properties influences strongly on the erosive wear [Kumar et al. 2020]. Improved microstructure and hardness resulted with reduced erosive wear of A356 alloy [More et al. 2019]. Heat treatment process not only alter the microstructure and mechanical properties, but also resulted with lesser erosive wear [Ramesh et al. 2009]. It was confirmed that, material properties associated with heat treatment process, erodent materials and their size, location angle of specimens, impact speed, erodent feed rate influences strongly on the erosive wear. Systematic study of aforementioned variables is of paramount importance not only to understand the process mechanics and dynamics but also to reduce erosive wear.

In recent years, Taguchi method has been used to study and analyze the variables such as erodent size, impingement angle and graphite fillers on erosive wear behavior of polymer composite [Prashanth, 2020]. Taguchi method was employed to analyze and optimize the parameters (impact velocity, impingement angle, erodent feed rate, and erodent particle size) influence the TiAlN-coated aluminium alloy [Kiragi et al. 2019a]. Suresh et al. studied the effect of filler materials, air jet velocity, temperature, and impingement angle on the erosive wear of glass reinforced epoxy composites using Taguchi method [Suresh et al. 2019]. Taguchi method optimize the parameters

(impact velocity, filler content, impingement angle, and slurry feed rate) that could results in reduced erosive wear of epoxy composite [Sharma et al. 2019]. From the above literature, Taguchi method can be effectively used to study, analyze and optimize the parameters that could results in reduced EW.

In the present work, Al 6113 alloy subjected to heat treatment process was used to study and analyze the factors (impact speed, scissor jack height, time) influencing the EW. Al_2O_3 particles are used as an erodent material. Taguchi L_{27} orthogonal array matrices was used for conducting experiments and perform parametric analysis. Surface plot analysis examine the erosive wear behavior with change in input variables. Regression equations are derive by expressing erosive wear as a mathematical function of input variables (impact speed, scissor jack height, time) for all angular location of cylindrical specimens. Statistical tests (i.e. coefficient of correlation and significance) are conducted to test both the parameter significance and adequacy of models developed. Desirability function approach (DFA) was applied to perform single and multiple objective optimizations of factors responsible for minimum EW of all angular location of cylindrical specimens.

2.0 Materials and Methods

The chemical composition of Al 6113 alloy is presented in Table 1. Al 6113 alloy possess weldable characteristics and are widely suitable for parts require assembly [Soboyejo et al. 2006]. The hard Al_2O_3 particles are used as an erodent material possessing approximately the size of 600 µm.

The schematic view of experimental set-up is shown in Fig. 1. Frame made up of stainless steel is the major part supports all other functional parts such as, motor, mechanical lifter, acrylic shaft and tank of experimental set-up (refer Fig. 1). A DC motor (specification: frequency 50 Hz, Power: 0.25 HP, Speed: 5000 rpm, and Voltage: 90V) rotates the acrylic shaft which has scrubbed screws to hold acrylic disc. The disc has drilled internal threaded holes to fasten the specimen at different orientations (0^o, 45^o and 90^o). Note that, the disc diameter is about 130 mm with a thickness of 20 mm. The testing specimen (Al 6113 age hardened alloy) of dimension 30 mm (which has 10 mm threaded to fasten the disc) was used. Note that as the shaft rotates the disc connected to shaft also rotates.

Table. 1 Chemical composition of 6113 alloy

Element	Si	Fe	Cu	Mn	Mg	Cr	Zn	Ti	Al
Wt. (%)	0.6-1.0	0.3	0.6-1.1	0.1-0.6	0.8-1.2	0.1	0.25	0.1	Bal.

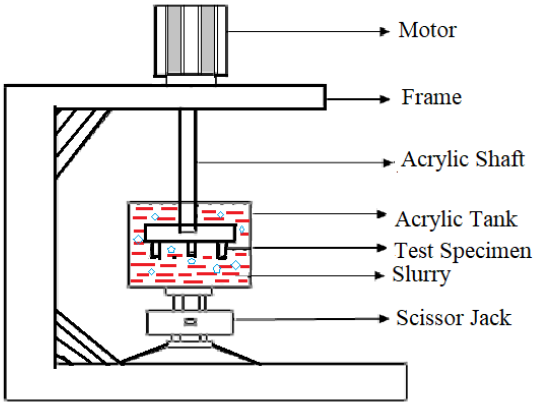

Fig. 1 Schematic view of experimental set-up

3.0 Experimental set-up

Experiments were carried out in a rotating slurry tank (H_2O + 5% HCL), wherein 20% Al_2O_3 particles of size ≈ 600 µm used as an erodent material. The slurry is rotating at three different angles with an impact speed of 500-1500 rpm. Mechanical lifter (i.e. scissor jack) of maximum lift capacity up to 250 mm, was used to ensure the immersion of test specimens completely in the slurry tank. Note that the impact of different height of mechanical lifter on the erosive behavior of samples are also tested. The impact of duration of test specimen suspended at different angles (0^o, 45^o and 90^o) in the rotating slurry tank during operation was examined on the erosive wear behavior of Al 6113 age hardened alloy. Table 2 present the control factors and their operating levels and are decided after consulting detailed literature review [Kiragi et al. 2019; Prashanth, 2020; Kiragi et al. 2019a].

The summary of experimental procedure is discussed below,

1. Prior to experiments the specimens were cleaned initially with warm water to remove any foreign materials or grease present on the surface. Later, the specimens were cleaned with acetone and air-dried.
2. Weight loss method is employed to measure the erosive wear behavior of Al 6113 age hardened alloy. Erosion wear measurements are carried out subjected to the specimens weighed before and after erosion tests with the help of digital weighing balance possessing a resolution 0.001 mg.

   The test specimens are held in the acrylic disc to achieve desired impingement set at different angles. The tank was filled with slurry wherein the specimens were ensured completely immersed. Stop watch was used to accurately monitor the duration of experiments. DC Motor was started and adjusted to the desired speed. After ensuring the completion of experiments the tests was stopped when the desired time is achieved.
3. The specimen was then removed, cleaned with acetone and dried to record the final mass. The percent of erosive wear is then calculated according to Eq. 1
4. Experiments are repeated to record the erosive wear with different speed, height and duration.

$$\text{Percentage of wear rate} = \frac{Intial\ \ mass - Final\ \ mass}{Intial\ \ mass} X100 \quad (1)$$

Table. 2 Input factors and levels

Control Factor	Symbols	Level (1, 2 and 3)
Impact Speed, rpm	A	500, 1000, 1500
Height, mm	B	140, 150, 160
Time, hrs	C	1, 2, 3

4.0 Results and discussions

The collected experimental input-output data are analyzed using analysis of variance and optimized using desirability function approach. Minitab 19 software platform used for the said purpose. The analysis of erosive wear of specimens mounted at different angles (0^o, 45^o and 90^o) are discussed below,

4.1 Parameter analysis

Taguchi L27 orthogonal array experiments are carried out with different sets of input variables (impact speed, height and time), wherein the erosive wear was measured subjected to specimen mounted at different impingement angles. The input-output data collected from experiments is presented in Table 3.Practical significance of each terms in Eq. [2-4] were tested at pre-set level of confidence at 95% (p-value <= 0.05). Results of analysis of variance tests are presented in Table 4. Important to note that, the terms (A, AA, and AB) are found significant for erosive wear behavior of specimens mounted at all angles (0^o, 45^o and 90^o). As their corresponding p-values are found to be less than 0.05. Square terms of impact speed are found significant for all responses (EW at all different angles 0^o, 45^o and 90^o) and their relationship is non-linear in nature (refer Fig. 2). The square terms of height and time was found insignificant (p-value > 0.05) and their relationship with EW for all specimens mounted at different angles (0^o, 45^o and 90^o) was found to be linear (refer Fig. 2). The individual terms (impact speed and height) were found significant for all responses (except, height for EW at 45^o**)** and their interaction term (impact speed and height, AB) is also found significant. In response Eq. 2-4, erosive wear value does not change much with the inclusion of insignificant or noncontributory terms. Note that, the models determined different significant and insignificant terms for the responses based on their input variable influence and also based on model fitness (refer Table 5). Note that, the correlation coefficient value also determines the best fit model. It is important to note that, the response equation correspond to EW at 90^o resulted with better correlation coefficient (R^2) value equal to 0.9411. Excluding insignificant terms (adjusted R^2 value = 0.05) in the response equation not only reduces the correlation coefficient value but also results in imprecise input-output relationship. Furthermore, prediction accuracy also reduces with removing insignificant terms from response Eq. 2-4. The specimens mounted at different impingement angles (0_o, 45_o and 90_o) wherein the erosive wear is expressed as a mathematical function of input variables (impact speed, height, and time) is given in Eq 2-4.

EW_0^0=-49+0.0428A+0.30B+35.7C-0.00036A^2-0.00139B^2-0.591C^2+0.000286AB-0.00311AC-0.1871BC (2)

EW_{45}^0=326+0.0181A-4.26B+24.8C-0.00039A^2+0.0125B^2+0.34C^2+0.000482AB-0.00147AC-0.15BC (3)

EW_{90}^0=-15+0.1513A-0.65B+29.6C-0.000049A^2+0.00306B^2+0.046C^2-0.000298AB+0.00042AC-0.1766BC (4)

Table. 3 Standards Orthogonal L_{27} Array of Taguchi for Erosive Wear

Sl. No.	Input Factors			Erosive Wear, gm		
	Impact Speed, rpm	Height, mm	Time, Hrs.	0˚	45˚	90˚
1	500	150	1	6.0	6.1	2.3
2	500	150	2	6.1	6.7	2.2
3	500	150	3	7.9	9.0	7.8
4	500	160	1	2.4	6.2	2.3
5	500	160	2	4.5	5.4	1.3
6	500	160	3	4.6	4.6	2.1
7	500	170	1	2.2	2.3	2.1
8	500	170	2	2.3	2.5	1.0
9	500	170	3	1.3	3.6	1.3
10	1000	150	1	17.5	19.8	16.3
11	1000	150	2	30.9	40.0	39.6
12	1000	150	3	43.2	42.8	39.4
13	1000	160	1	13.6	15.1	12.3
14	1000	160	2	22.5	24.6	18.2
15	1000	160	3	21.1	25.0	20.5
16	1000	170	1	5.20	9.3	3.80
17	1000	170	2	6.80	19.9	8.8
18	1000	170	3	12.40	18.7	17.8
19	1500	150	1	16.25	18.1	11.0
20	1500	150	2	12.88	18.0	12.0
21	1500	150	3	9.20	11.9	9.0
22	1500	160	1	18.05	22.0	18.01
23	1500	160	2	13.9	14	13.5
24	1500	160	3	11.82	12	11
25	1500	170	1	15.8	26.7	5.8
26	1500	170	2	17.3	21.6	4.7
27	1500	170	3	10.9	32.5	4.3

Table. 4 ANOVA table for the response EW of specimens located at different angle

Source	DF	EW at 0^0		EW at 45^0		EW at 90^0	
		Adj. SS	P-Value	Adj. SS	P-Value	Adj. SS	P-Value
Model	9	1151.01	0.000	1701.49	0.000	1451.86	0.000
Linear	3	564.15	0.000	1028.26	0.000	502.08	0.000

A	1	465.12	0.000	1006.51	0.000	245.75	0.000
B	1	97.21	0.000	12.07	**0.289**	185.60	0.000
C	1	1.82	**0.556**	9.68	**0.341**	70.73	0.002
Square	3	491.22	0.000	570.18	0.000	885.25	0.000
AA	1	489.00	0.000	560.15	0.000	884.68	0.000
BB	1	0.12	**0.881**	09.34	**0.350**	0.56	**0.750**
CC	1	2.10	**0.528**	0.68	**0.798**	0.01	**0.962**
2-IT	3	95.65	0.004	103.05	0.042	64.52	0.025
AB	1	24.57	0.041	69.60	0.018	26.58	0.040
AC	1	29.08	0.028	6.45	**0.435**	0.53	**0.758**
BC	1	42.00	0.010	27.00	**0.120**	37.42	0.017
Error	17	85.82		171.64		90.89	
Total	26	1236.83		1873.13		1542.75	

Table. 5 Statistical tests (significance and coefficient of correlation) for EW

Tests	**Details**	**EW-0^0**	**EW-45^0**	**EW-90^0**
Correlation coefficient	R^2 value (%)	93.06	90.84	94.11
	Adjusted R^2 (%)	89.39	85.99	90.99
Statistical test	Significant terms (P-Value <= 0.05)	A, B, AB, AA, AB, AC, BC	A, AA, AB	A, B, C, AA, AB, BC
	Insignificant terms (P-Value > 0.05)	C, BB, CC	B, C, BC, BB, CC, AC, BC	BB, CC, AC

4.2 Surface plot analysis

Three-dimensional surface plots are drawn which represents the erosive wear behavior with change in input variables (impact speed, height and time). Two variables were varied simultaneously after keeping the rest at their fixed middle value. The following observations are made from the analysis,

1. EW showed increasing trend up to the mid-values of impact speed and thereafter decreases (refer Fig. 2 a, d, g). Height of rotating slurry tank showed a linear relationship with EW. Impact speed increases the erosive wear due to increased speed of rotating disc and thereby creates whirling effect which hits Al_2O_3 particles at higher velocity on the Al 6113 material as a result of kinetic energy phenomenon. Beyond the critical impact speed, EW decreases due to the increased possibility of fragmentation of erodent material (i.e. Al_2O_3 particles) itself and also it's associated kinetic energy. Although EW do not show significant change with slurry tank height for specimens mounted at 0^0 and 45^0, but there is a linear decreasing trend was observed for specimen mounted at 90^0. EW decreases with increase in mechanical scissor height is attributed to increased severity of Al_2O_3 particles attack on specimen causes initially deep craters at low height, later at higher height the solid particles deposited in and around the affected regions and

thereby do not enable the specimen to cause further wear.

2. Fig. 2 (b, e, h) show the erosive wear of Al 6113 specimens with varied height and time. EW was seen to increase initially with impact speed and after crossing the mid-values it decreases. Note that, the impact of the time is seen to have almost negligible and is truly consistent with the significance test results (refer Table 5). As the time progress the kinetic energy associated with hard particles striking the target material causes damage on the targeted specimen surface initially and later with continuous striking of hard Al_2O_3 particles the material undergoes plastic deformation and strain hardening which often resists erosion.

3. EW behavior with height and time is presented in Fig. 2 (c, f and i). Increase in height showed decrease in EW and negligible change with EW with change in time. It is also observed that there exists a linear relationship with both height and time. The resulted linear relationship is in consistent with the statistical test results.

The major conclusions drawn from the surface plots are as follows, a) Impact speed found to have major contribution followed by height and time (refer Table 4). The interaction terms (impact speed and height) were found to have significant influence on EW. There is a negligible impact of interaction terms (AC: impact speed and time; BC: height and time) compared to interaction factor effects (i.e. AB: impact speed and height). The resulted surface plots are in consistent with the statistical test results (refer Table 4 and 5).

4.3 Desirability Function Approach (DFA)

DFA is applied to determine the optimal set of factors (impact speed, height, and duration) that could results in reduced erosive wear of samples mounted at different angles (0^o, 45^o and 90^o). DFA showed their success in optimizing both individual and multiple responses to obtain better quality in manufactured parts. In this approach, the actual outputs are converted to a scale-free value refers to desirability (d). Desirability values vary in the ranges between 0 and 1, which decides the estimated output quality. The desirability value i.e. d = 0 or close to 0, depicts it is completely undesirable or local

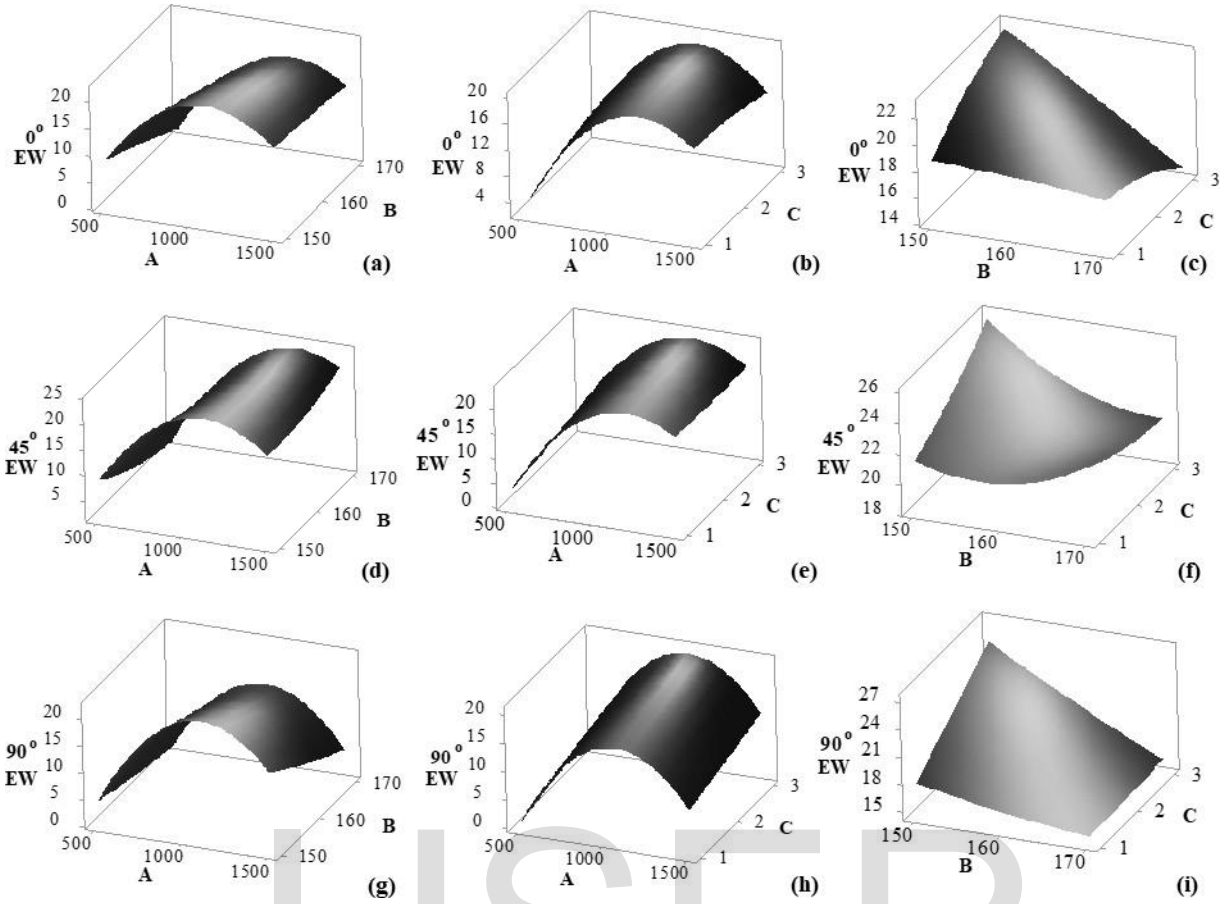

Fig. 2 Surface plots of EW at 0^o specimen angle (a-c), 45^o specimen angle (d-f), 90^o specimen angle (g-i) with: a, d, g) speed and height; b, e, h) speed and time; c, f, i) height and time

solution, whereas d = 1 or close to unity which corresponds to the output value close to an ideal solution. For performing multiple-objective optimization, the composite or overall desirability (D_o) value was estimated after taking in to account of all the geometric mean of individual desirability. The factor setting corresponds to single and multiple objective optimizations of erosive wear behaviour of specimens placed at different angles (refer Fig. 3-4). From Fig. 3 a-c, it was observed the lesser erosive wear of test samples (Al 6113 age-hardened alloy) was observed when the specimen mounted at 90^o. The results are in consistent with the earlier research reports [Kirols et al. 2017; Raj et al. 2018]. At higher angles, there is a greater resistance to strong intermetallic crack as a result of opposed normal stresses leads to the material detached in the form of spalts rather than ploughing or chips. A steady increase in erosive wear was observed with increase in experimental duration (i.e. 3 hrs.) at higher impingement angle (i.e. 90^o). This might be due to the impact of Al_2O_3 particles striking the target (i.e. Al 6113 age hardened) material increases as the time progresses which results in increased wear (Fig. 3). EW decreases with

increase in scissor jack height (i.e. from 150 to 170 mm), wherein the hard Al_2O_3 particles hit the target specimen creates deep craters at lower height and the hard-solid particles get deposited in that region which offer greater resistance to wear.

The erosive wear corresponds to single objective optimization for the specimen mounted at different angles i.e. 0.5258 g for 90^0, 2.1183 g for 45^0 and 0.6426 g for 0^0. Input variables (impact speed, height and time) correspond to minimum erosive wear at different specimen angles was presented in Table 6. Note that at higher specimen angle (i.e. 90^0) resulted with minimum EW, might be due to the greater resistance to offer strong intermetallic crack as a result of opposed strong normal stresses.

Multi-objective optimization offers many solutions and the resulted solutions are dependent on the weights or relative importance assigned to each response. In the present work, equal weights (0.333 for 0^0, 0.333 for 45^0 and 0.333 for 90^0) are assigned for each response and resulted optimal input and output values are presented in Table 6. EW of 0.9641 g, 2.2963 g, and 0.8536 g was obtained for the specimen mounted at 0^0, 45^0 and 90^0 angles, respectively (refer Fig. 4). The input values such as impact speed of 500 rpm, scissor jack height of 170 mm and time of 1.3232 hr resulted with minimum EW. Note that, overall desirability value was found equal to 1, which dictates the determined solution is treated to global solution always.

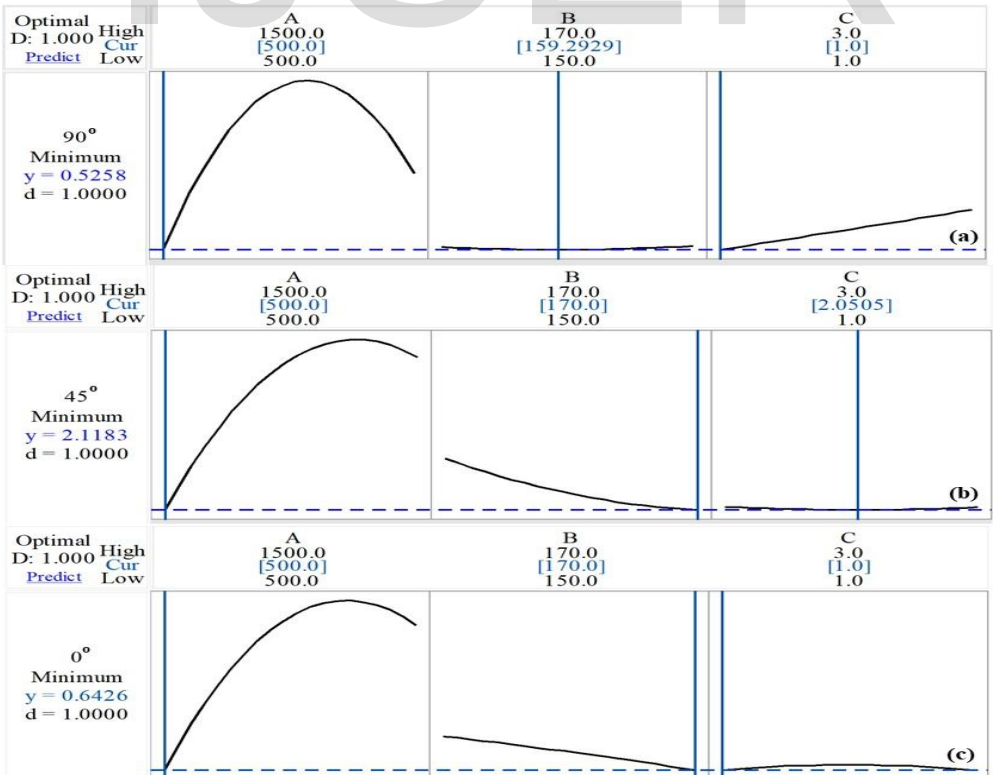

Fig. 3 Single objective optimization for the specimen mounted at: a) 90^0, b) 45^0 and c) 0^0

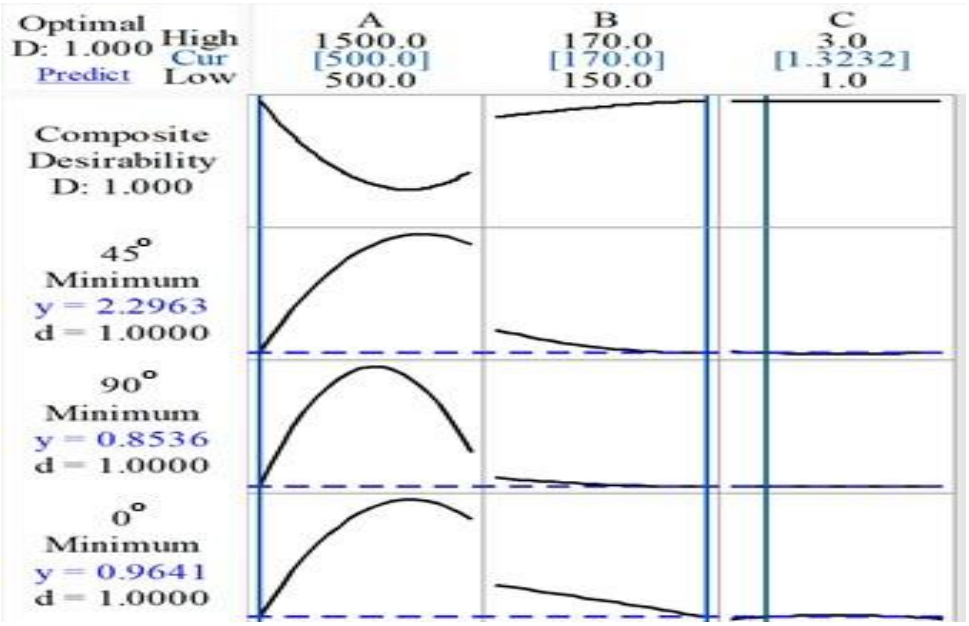

Fig. 4 Multiple objective optimizations for the entire specimen mounted at different angles

Table 6 Summary results of single and multiple objective optimizations for minimum EW

Optimization	**EW at 0^0 (Input & output)**	**EW at 45^0 (Input & output)**	**EW at 90^0 (Input & output)**
Single-objective	EW: 0.6426 gm Impact speed: 500 rpm Height: 170 mm Time: 1 hr	EW: 2.1183 g Impact speed: 500 rpm Height: 170 mm Time: 2.0505 hr	EW: 0.5258 g Impact speed: 500 rpm Height: 159.293 mm Time: 1 hr
Multiple-objective	EW: 0.9641 gm	EW: 2.2963 gm	EW: 0.8536 gm
	Impact speed: 500 rpm; Height: 170 mm; Time: 1.3232 hr		

5.0 Conclusions

Taguchi L_{27} orthogonal array experiments are carried out for parametric analysis and optimization for minimum EW of Al 6113 age hardened alloy is as follows,

1. Input variables (impact speed, height and time) are treated as inputs to know their EW of specimens mounted at different angles (0^0, 45^0 and 90^0). Impact speed found to have maximum contribution followed by scissor jack height and time. The interaction factor (AB: impact speed and scissor height) effects found to be significant at preset 95% confidence level with maximum contributions. The impact of other interaction terms (BC: scissor jack height and time; AC: impact speed and time) were found insignificant towards EW.

2. The square terms of impact speed are found to be significant which indicates their relationship with EW was found to be non-linear. The relationship of EW with scissor jack height and time was found to be insignificant and are found to be linear. Surface plot analysis are in consistent with the results obtained from statistical results.

3. The coefficient of correlation determined for EW of specimens mounted at different angles were found equal to 0.9306 for 0^0, 0.9084 for 45^0 and 0.9411 for 90^0, respectively. It was also noted that, better correlation coefficient value was observed for specimen mounted at an angle equal to 90^0. The correlation coefficient value close to unity indicates the best fit model for performing better prediction and optimization.

4. DFA was applied to perform single and multiple objective optimizations of specimens mounted at different angles (0^0, 45^0 and 90^0). The desired minimum EW of 0.5258 g was obtained for the specimen mounted at 90^0 angle. Simultaneous optimization of multiple responses for minimum EW for all the specimens mounted at different angles are performed. Note that, Input values such as impact speed 500 rpm, scissor jack height of 170 mm, and time of 1.3232 hr resulted with a minimum EW of 0.9641 g, 2.2963 g, and 0.8536 g was obtained for the specimen mounted at 0^0, 45^0 and 90^0 angles, respectively. At low values of impact speed, the hard Al_2O_3 particles striking the target material at lower velocity creating lesser damage resulted with less EW. Increase in scissor jack height creates damage and crack initially and the erodent material get stuck at the damaged region which offer greater resistance to wear. As time progress the hard Al_2O_3 particles hitting the target material increases and thereby undergoes plastic deformation and removes material in the form of spalts upto 1.3232 hrs, and latter creates crack and increases wear.

References

[1] Clark, H. M., & Wong, K. K. (1995). Impact angle, particle energy and mass loss in erosion by dilute slurries. *Wear*, 186, 454-464.

[2] Davis, J.R. (1993). *Aluminum and aluminum alloys*. ASM international.

[3] Desale, G. R., Gandhi, B. K., & Jain, S. C. (2009). Particle size effects on the slurry erosion of aluminium alloy (AA 6063). *Wear*, *266*(11-12), 1066-1071.

[4] Dursun, T., & Soutis, C. (2014). Recent developments in advanced aircraft aluminium alloys. *Materials & Design (1980-2015)*, *56*, 862-871.

[5] Elmidany, T. T. M., Abdel-Samad, A. A. F., Abdel Moneim, A. M. G., & Saleh, Y. S. A. A. (2020). Effect of Material Type, Impact Angle and Specimen Shape on Erosion Process. *Bulletin of the Faculty of Engineering. Mansoura University*, 41(2), 1-8.

[6] Harsha, A. P., & Bhaskar, D. K. (2008). Solid particle erosion behaviour of ferrous and non- ferrous materials and correlation of erosion data with erosion models. *Materials & Design*, *29*(9), 1745-1754.

[7] Kiragi, V. R., & Patnaik, A. (2019). Erosive wear behaviour of aluminium alloys: a comparison between slurry and dry erosion. *Materials Research Express*, *6*(8), 086503.

[8] Kiragi, V. R., Patnaik, A., Singh, T., & Fekete, G. (2019a). Parametric optimization of erosive wear response of TiAlN-coated aluminium alloy using Taguchi method. *Journal of Materials Engineering and Performance*, *28*(2), 838-851.

[9] Kirols, H. S., et al. "Water droplet erosion of stainless steel steam turbine blades." *Materials Research Express* 4.8 (2017): 086510.

[10] Kumar, G. V., Rao, C. S. P., & Selvaraj,

N. (2011). Mechanical and tribological behavior of particulate reinforced aluminum metal matrix composites–a review. *Journal of minerals and materials characterization and engineering*, *10*(01), 59.

[11] Kumar, N., & Mishra, S. (2020). Slurry erosion: An overview. *Materials Today: Proceedings*, 25, 659-663.

[12] More, S. R., Bhatt, D. V., & Menghani, J. V. (2019). Effect of microstructure and hardness on slurry erosion behaviour of A356 alloy using slurry pot test rig. *Transactions of the Indian Institute of Metals*, 72(12), 3191-3199.

[13] Patel GC, M., NB, P., HM, H., & Shettigar, A. K. (2020). Experimental analysis and optimization of plasma spray parameters on microhardness and wear loss of Mo-Ni-Cr coated super duplex stainless steel. *Australian Journal of Mechanical Engineering*, 1-14.

[14] Prashanth, N. (2020, January). Influence of erodent size, impingement angle and fillers on solid particle erosion wear behaviour of carbon fiber reinforced epoxy composite. In *AIP Conference Proceedings* (Vol. 2204, No. 1, p. 040020). AIP Publishing LLC.

[15] Raj, R. Rethan, and H. Kanagasabapathy. "Influence of abrasive water jet machining parameter on performance characteristics of AA7075-ZrSiO4-hBN hybrid metal matrix composites." *Materials Research Express* 5.10 (2018): 106509.

[16] Ramesh, C. S., Keshavamurthy, R., Channabasappa, B. H., & Pramod, S. (2009). Influence of heat treatment on slurry erosive wear resistance of Al6061 alloy. *Materials & Design*, 30(9), 3713-3722.

[17] Sharma, A., Kiragi, V. R., Choudhary, M., Biswas, S. K., & Patnaik, A. (2019). Slurry erosion behaviour of marble powder filled needle punched nonwoven reinforced epoxy composite: an optimization using Taguchi approach. *Materials Research Express*, *6*(10), 105318.

[18] Soboyejo, W. O., & Srivatsan, T. S. (Eds.). (2006). *Advanced structural materials: properties, design optimization, and applications*. CRC press.p.528. https://doi.org/10.1201/9781420017 465

[19] Suresh, J. S., Devi, M. P., & Sasidhar, M. (2019). Assessment of solid particle erosive wear of glass reinforced epoxy hybrid composites using Taguchi approach. *Materials Today: Proceedings*, *18*, 342-349.